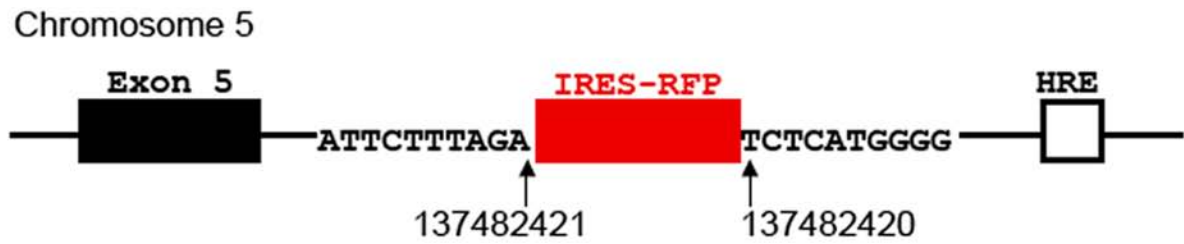
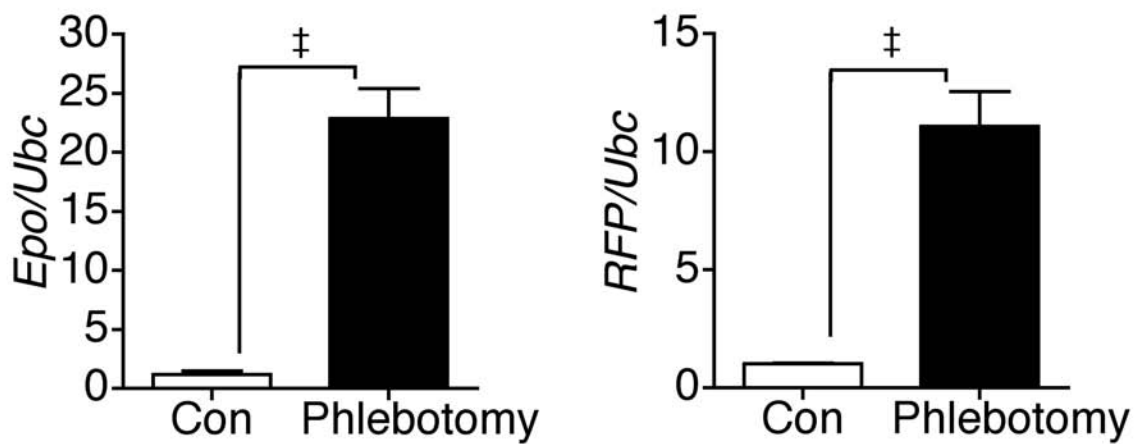


Chang et al. Supplemental Materials

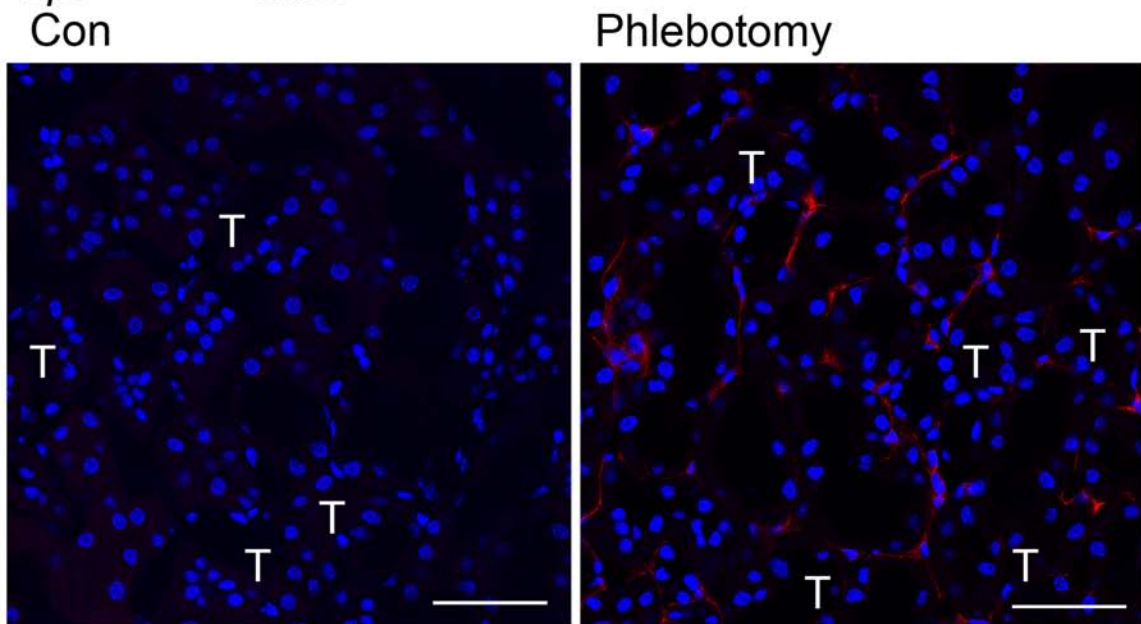
A



B *Epo*^{IRES-RFP/+} mice



C *Epo*^{IRES-RFP/+} mice



Epo-RFP nuclei

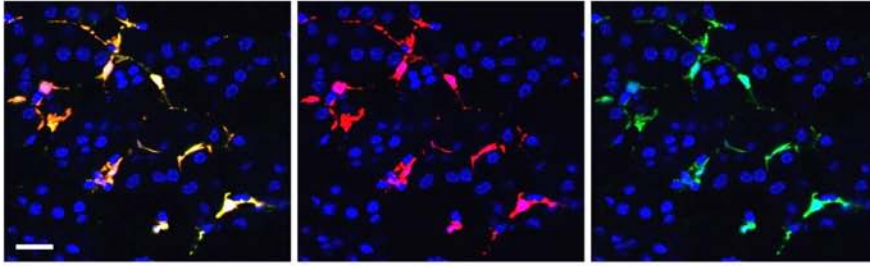
Epo-RFP nuclei

Fig. S1

Supplemental Figure 1. Epo-RFP⁺ cells faithfully identify renal erythropoietin-producing cells. (A) *Epo*^{IRES-RFP/+} mice on the C57BL/6 background were generated by knocking *IRES-RFP* between 13432 and 13433 at *Epo* 3'-UTR of chromosome 5 (Ensembl ENSMUSG00000029711). (B) Relative expression of renal *Epo* and *RFP* transcripts in mice without (Con) and after phlebotomy. Phlebotomy was performed one day before analysis. n = 5/group. ‡*P*<0.001. (C) Confocal images of the kidney sections showing Epo-RFP⁺ cells in peritubular interstitium. Original magnification, x400. Scale bar, 50 μm.

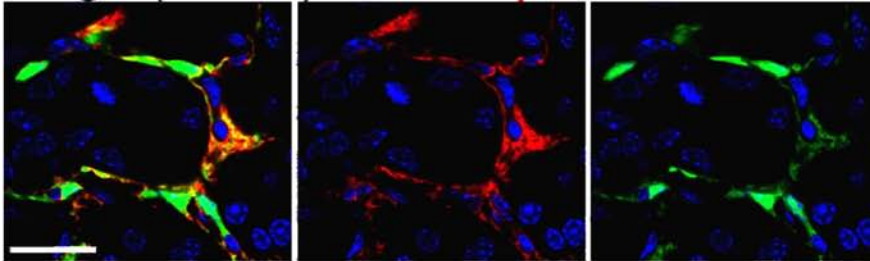
A *Foxd1*^{Cre/+}; *Rs26*^{fstdTomato/+}; *Col1a1-GFP*^{Tg} mice

Merge (nuclei) Foxd1-RFP Col1a1-GFP

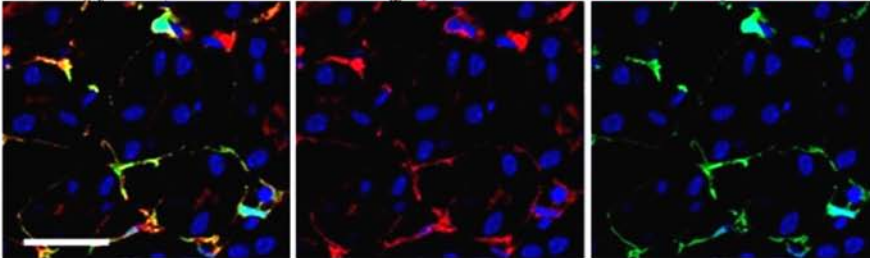


B *Col1a1-GFP*^{Tg} mice

Merge (nuclei) PDGFR β Col1a1-GFP



Merge (nuclei) CD73 Col1a1-GFP



Merge (nuclei) p75 Col1a1-GFP

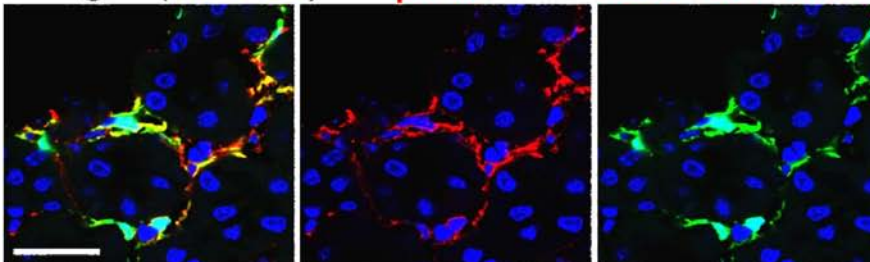


Fig. S2

Supplemental Figure 2. Kidney *Col1a1-GFP*⁺ pericytes are *Foxd1*-derived, *PDGFR* β ⁺, *CD73*⁺, and *p75*⁺ cells. (A) Confocal images of the kidney sections of

Foxd1^{Cre/+}; *Rs26*^{efsdTomato/+}; *Col1a1-GFP*^{Tg} mice. (B) Confocal images of staining for platelet-derived growth factor receptor β (PDGFR β), CD73 (or 5'-nucleotidase) and p75 nerve growth factor receptor on the kidney sections of *Col1a1-GFP*^{Tg} mice. Original magnification, x400. Scale bar, 20 μ m.

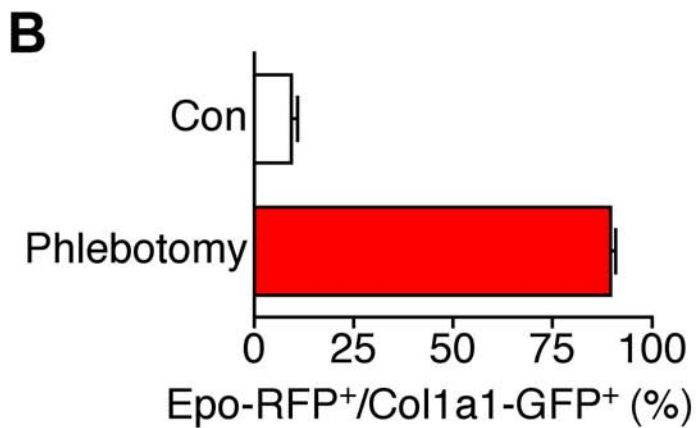
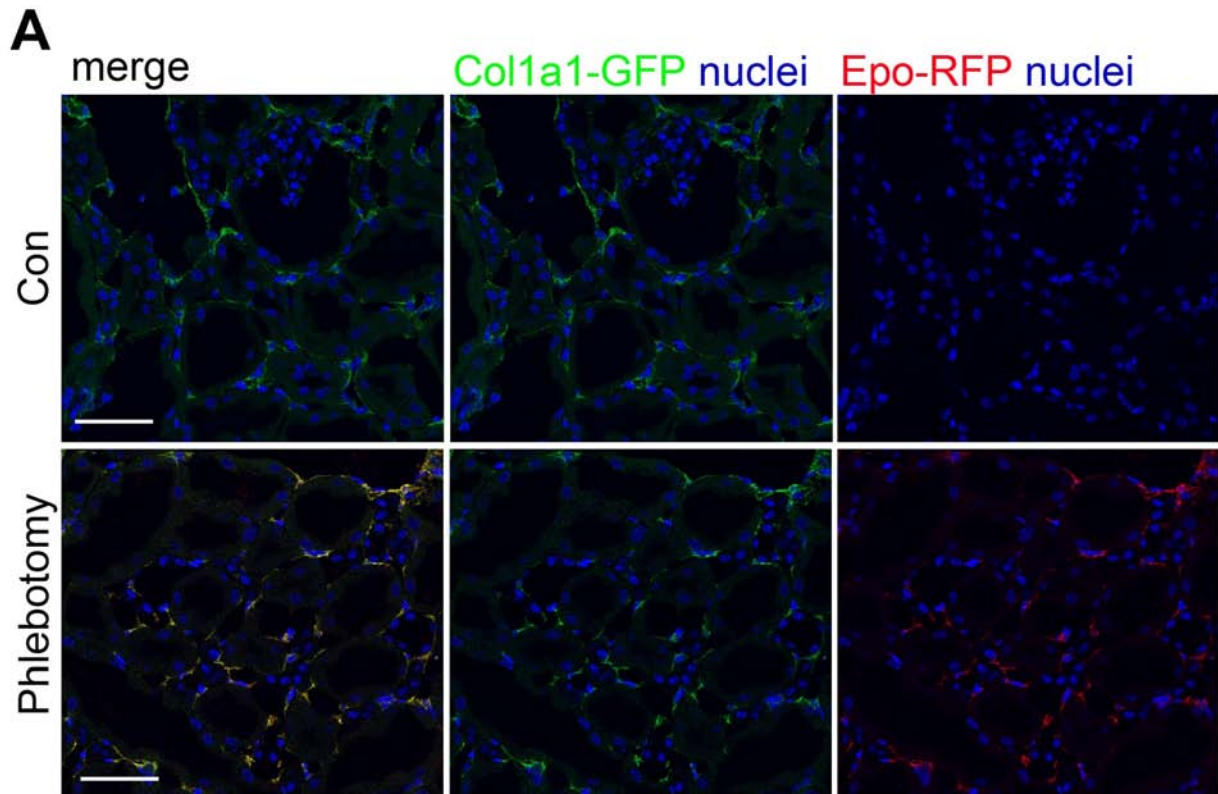


Fig. S3

Supplemental Figure 3. Kidney *Col1a1-GFP*⁺ pericytes express erythropoietin. (A) Confocal

images of the kidney sections of *Epo^{IRE5-RFP/+};Colla1-GFP^{Tg}* mice without (Con) and after phlebotomy. Original magnification, x400. Scale bar, 50 μ m. (B) The graph showing the percentage of Colla1-GFP⁺ kidney pericytes with Epo-RFP expression. Data are expressed as means \pm s.e.m. n = 5/group.

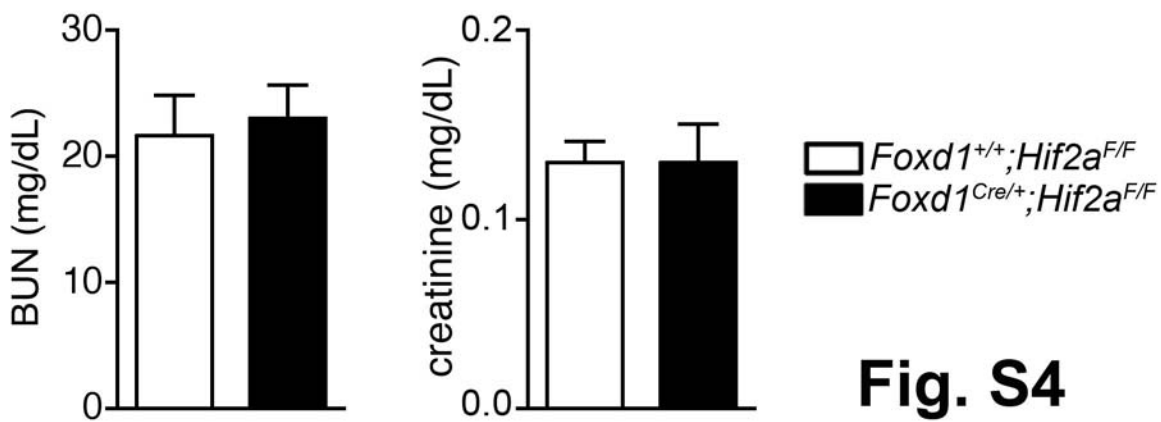
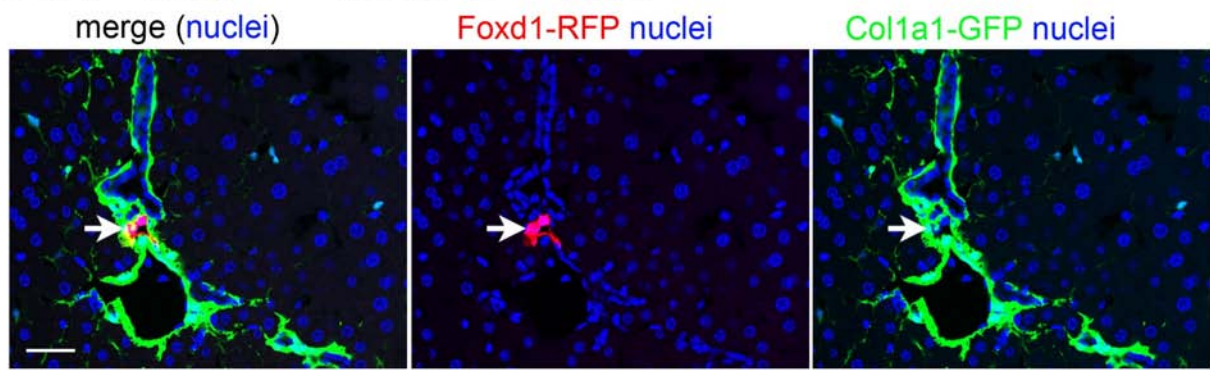


Fig. S4

Supplemental Figure 4. Plasma levels of blood urea nitrogen (BUN) and creatinine of adult *Foxd1^{+/+};Hif2a^{F/F}* and *Foxd1^{Cre/+};Hif2a^{F/F}* mice. Student's t-test was used for data analyses. n = 10/group.

A *Foxd1^{Cre/+};Rs26^{stdTomato/+};Col1a1-GFP^{Tg}* mouse



B

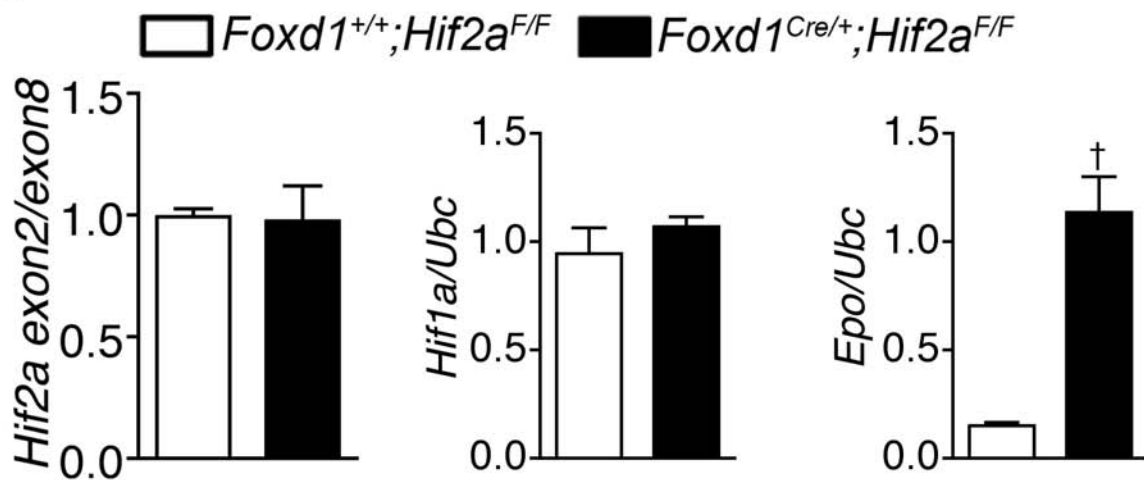


Fig. S5

Supplemental Figure 5. Hepatic erythropoietin expression increases in *Foxd1^{Cre/+};Hif2a^{F/F}* mice.

(A) Confocal images of the liver section of *Foxd1^{Cre/+};Rs26^{stdTomato/+};Col1a1-GFP^{Tg}* mice. Arrow indicates Foxd1-RFP⁺ vascular smooth muscle cells of hepatic arteries. Original magnification, x400. Scale bar, 20 μ m. (B) Expression of *Hif2a*, *Hif1a* and *Epo* in livers of *Foxd1^{+/+};Hif2a^{F/F}* and *Foxd1^{Cre/+};Hif2a^{F/F}* mice. Student's t-test was used for data analyses. n = 10/group. [†]*P*<0.01.

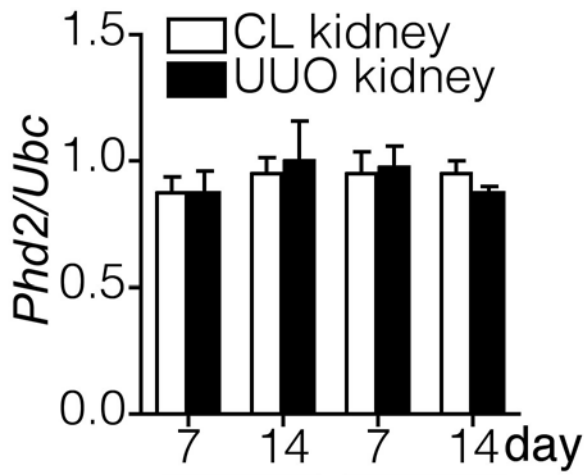


Fig. S6 Con Phlebotomy

Supplemental Figure 6. Expression of *prolyl hydroxylase 2* in controlateral (CL) and unilateral ureteral obstruction (UUO) kidneys of mice subjected to phlebotomy or not (Con) one day before analyses. One-way ANOVA was used for data analyses. n = 10/group/time point.

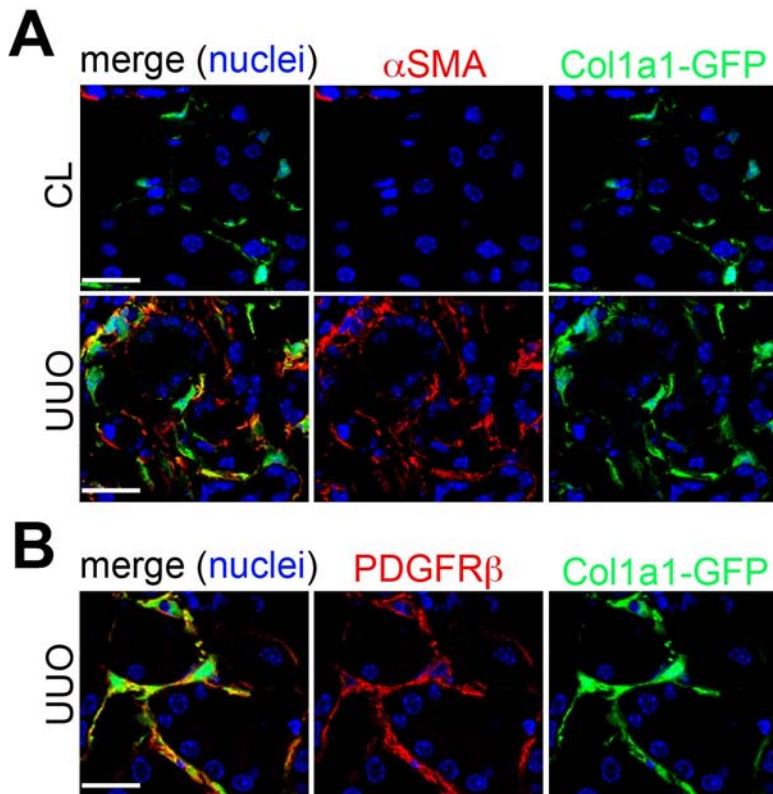


Fig. S7

Supplemental Figure 7. Pericytes differentiate to α smooth muscle actin⁺ myofibroblasts that retain platelet-derived growth factor receptor β expression in kidneys after unilateral ureteral obstruction surgery. (A) Confocal images of α smooth muscle actin (α SMA) staining on CL and UUO kidney sections of *Col1a1-GFP^{Tg}* mice at day 7 after surgery. (B) Confocal images of PDGFR β staining on UUO kidney sections of *Col1a1-GFP^{Tg}* mice at day 7 after surgery. Original magnification, x400. Scale bar, 20 μ m.

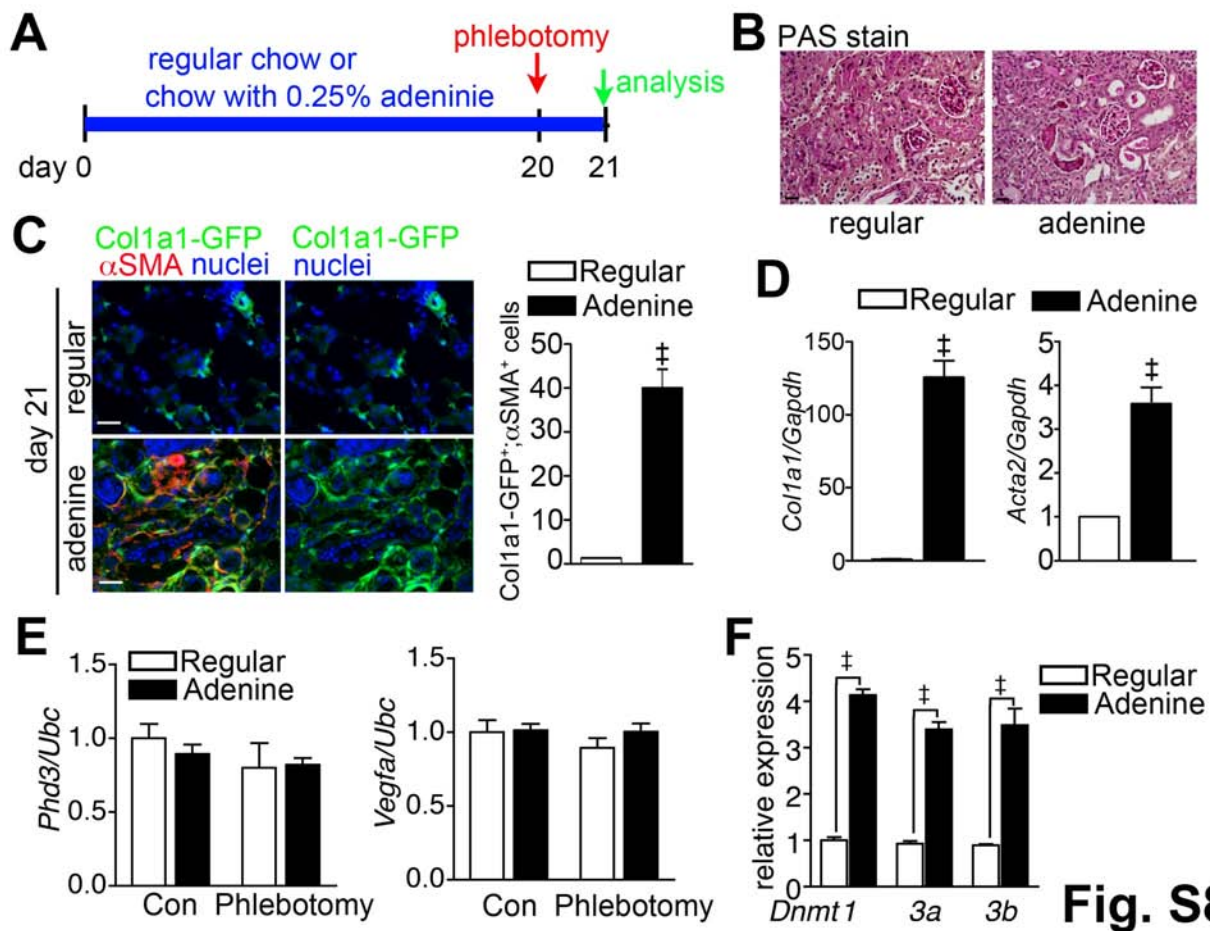


Fig. S8

Supplemental Figure 8. Mouse model of adenine-induced nephropathy. (A) Schema for adenine-induced nephropathy. (B) Periodic acid-Schiff (PAS) stain on kidney sections of mice fed

with regular or adenine chow. (C) Representative images of α SMA staining on kidney sections of *Coll1a1-GFP^{Tg}* mice fed with regular or adenine chow. Cell numbers of α SMA⁺;Coll1a1-GFP⁺ myofibroblasts per field at X400 magnification are shown in bar chart. (D) Renal expression of *Coll1a1* and *Acta2* of mice fed with regular or adenine chow. (E) Renal expression of *Phd3* and *Vegfa* of mice fed with regular or adenine chow without (Con) or after phlebotomy. (F) Renal expression of *Dnmt* isoforms of mice with regular or adenine chow. Original magnification, x400. Scale bar, 20 μ m. Student's t-test and one-way ANOVA were used for analyses of data in (C, D) and (E, F) respectively. n = 10/group. [‡]*P*<0.001.

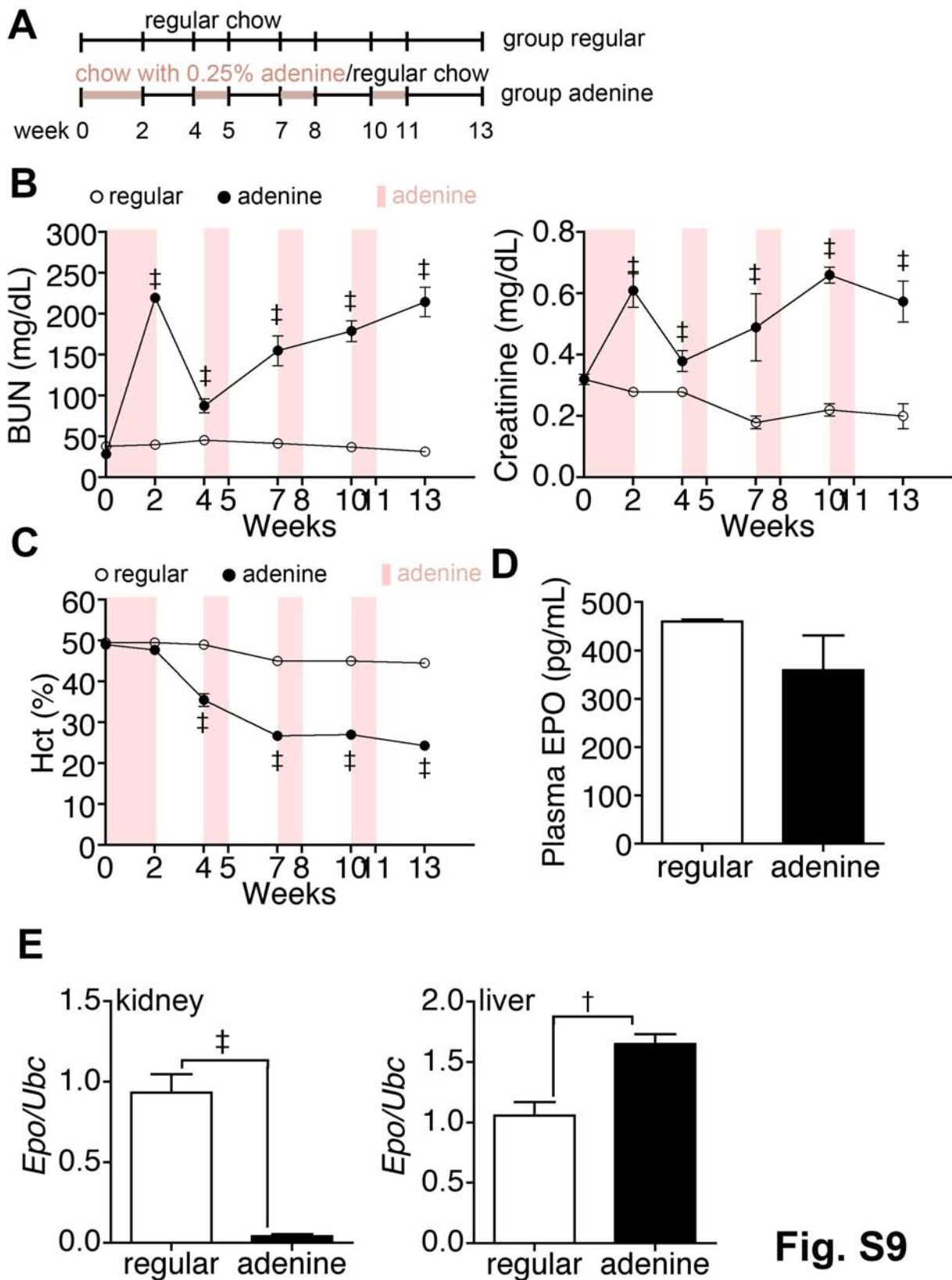


Fig. S9

Supplemental Figure 9. Anemia in mouse model of chronic adenine-induced nephropathy. (A)

Schema illustrating the feeding protocol of alternate administration of regular and

adenine-containing chows for mouse model of chronic kidney disease. (B, C) Plasma levels of BUN, creatinine and Hct at time points as indicated. (D) Plasma EPO levels of mice at 13 weeks after regular or adenine chow feeding. (E) *Epo* expression in kidney and liver of mice at 13 weeks after regular or adenine chow feeding. Student's t-test was used for data analyses between groups at each time point. n = 10/group. [†]*P*<0.01, [‡]*P*<0.001.

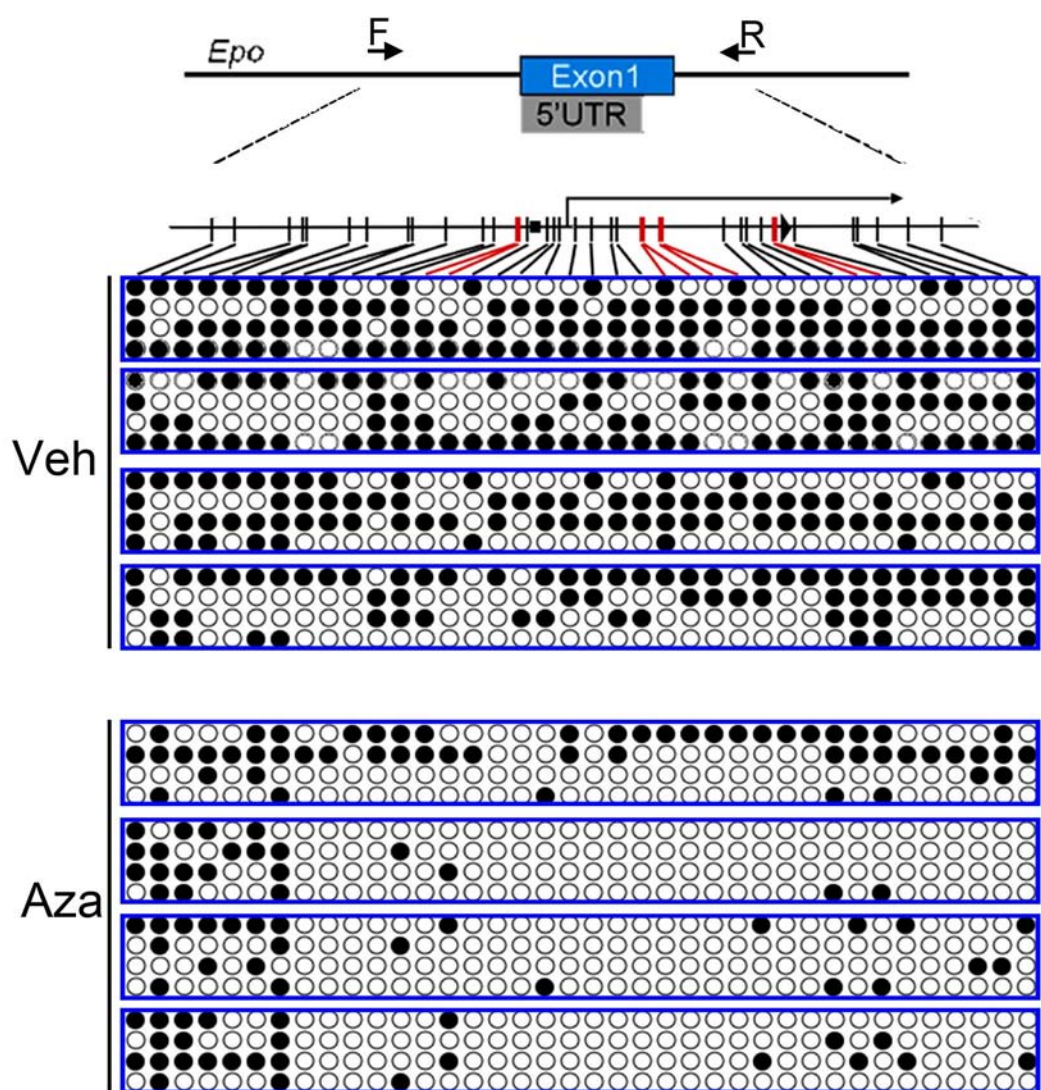
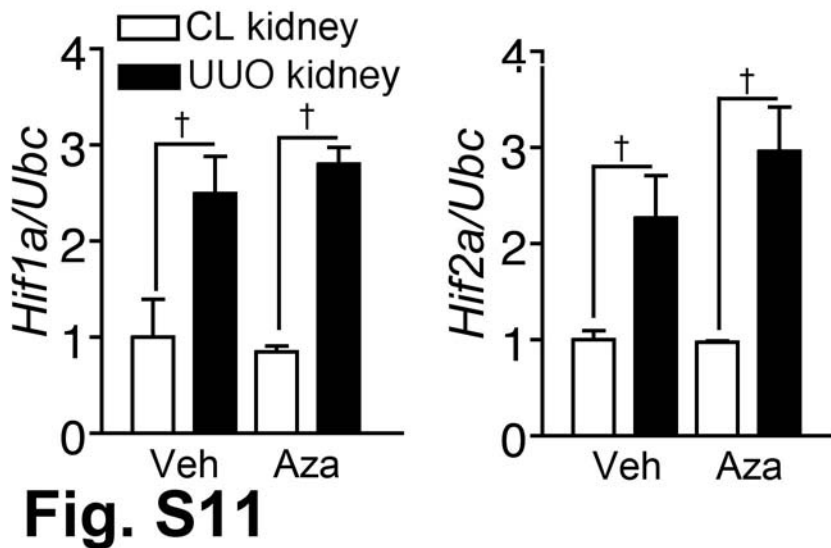


Fig. S10

Supplemental Figure 10. 5-azacytidine attenuates hypermethylation of *erythropoietin*

5'-untranslated region in kidney myofibroblasts. Bisulfite-converted genomic DNA was prepared from *Col1a1-GFP⁺;PDGFR β ⁺* myofibroblasts isolated from day 14 UUO kidneys of *Col1a1-GFP^{Tg}* mice with treatment of vehicle (Veh) or 5-azacytidine (Aza) indicated in **Figure 6C**. Each box is the bisulfite genomic sequencing of 5'-UTR amplified using primers indicated in **Figure 4A**; each row represents a single sequenced clone (four clones for each mouse); each dot is representative of a single CpG.



Supplemental Figure 11. 5-azacytidine does not affect the expression of hypoxia-inducible factors in kidneys. Renal expression of *Hif1a* and *Hif2a* in mice after UUO surgery with Veh or Aza treatment according to the schema in **Figure 6C**. One-way ANOVA was used for data analyses.

† $P < 0.01$. n = 10/group.

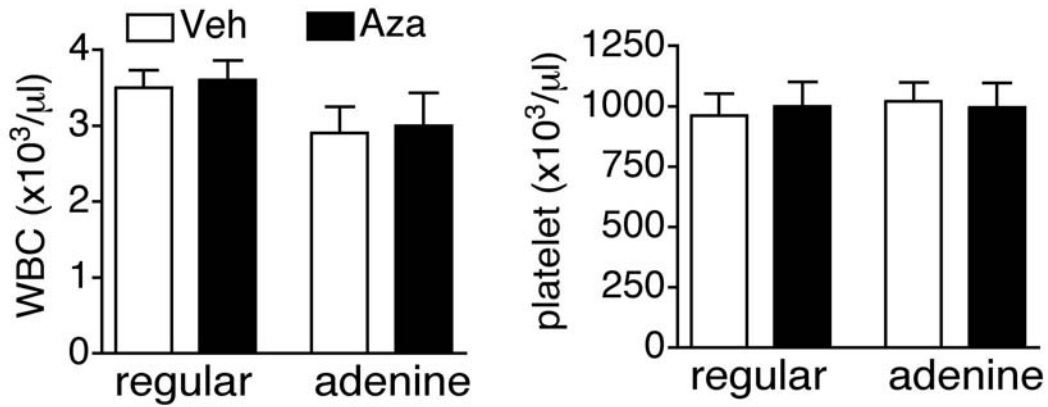


Fig. S12

Supplementary Figure 12. White blood cell (WBC) and platelet counts in peripheral blood of mice fed with regular or adenine chow. The protocol for mice fed with regular or adenine chow and receiving Veh or Aza treatment is shown in **Supplemental Figure 9A** and **Figure 7A**. One-way ANOVA was used for data analyses. $n = 12/\text{group}$.

Supplementary Table 1. Primer sequences used in quantitative polymerase chain reaction

Gene		Sequences
<i>Epo</i>	Forward	5'-CCA CCC TGC TGC TTT TAC TC-3'
	Reverse	5'-CTC AGT CTG GGA CCT TCT GC-3'
<i>Hif1a</i>	Forward	5'-ACA ACG CGG GCA CCG ATT CG-3'
	Reverse	5'-GCT CAC ATT GTG GGG AAG TGG C-3'
<i>Hif2a</i>	Forward	5'-GGG CCA CGG CGA CAA TGA CA-3'
	Reverse	5'-GCT GAT GGC CAG GCG CAT GA-3'
<i>Dnmt1</i>	Forward	5'-CGG CTC AAA GAC TTG GAA AG-3'
	Reverse	5'-TAG CCA GGT AGC CTT CCT CA-3'
<i>Dnmt3a</i>	Forward	5'-ACC AGG CCA CCT ACA ACA AG-3'
	Reverse	5'-TGC TTG TTC TGC ACT TCC AC-3'
<i>Dnmt3b</i>	Forward	5'-ACT TGG TGA TTG GTG GAA GC-3'
	Reverse	5'-CCA GAA GAA TGG ACG GTT GT-3'
<i>Phd2</i>	Forward	5'-GCG GGA AGC TGG GCA ACT ACA-3'
	Reverse	5'-CAT AGC CTG TTC CGT TGC CTG GG-3'
<i>Phd3</i>	Forward	5'-TCG CTT CCT CCC GAA CTC T-3'
	Reverse	5'-CAG AAA CGA GGG TGG CTA ACT T-3'
<i>Vegfa</i>	Forward	5'-ATC TTC AAG CCG TCC TGT GT-3'
	Reverse	5'-GCA TTC ACA TCT GCT GTG CT-3'
<i>Coll1a1</i>	Forward	5'-GAG CGG AGA GTA CTG GAT CG-3'
	Reverse	5'-GTT CGG GCT GAT GTA CCA GT-3'
<i>Acta2</i>	Forward	5'-CTG ACA GAG GCA CCA CTG AA-3'
	Reverse	5'-CAT CTC CAG AGT CCA GCA CA-3'

<i>Gapdh</i>	Forward	5'-ACG GCC GCA TCT TCT TGT GCA-3'
	Reverse	5'-AAT GGC AGC CCT GGT GAC CA-3'
<i>Hif2a, exon2</i>	Forward	5'-CAA TGA CAG CTG ACA AGG AGA-3'
	Reverse	5'-GGC AAC TCA TGA GCC AAC TC-3'
<i>Hif2a, exon8</i>	Forward	5'-GGA GCT ACT TGG ACG CTC TG-3'
	Reverse	5'-CTC CGT GTT TGG CTA GCA TC-3'
<i>Ubc</i>	Forward	5'-TCT CTG GAC GCC ACC GTG AAA C-3'
	Reverse	5'-GGC CAT CTT CCA GCT GCT TGC C-3'
<i>RFP</i>	Forward	5'-AGA AAA CAC TCG GCT GGG AG-3'
	Reverse	5'-GGT CCA CAT AGT AGA CGC CG-3'

Supplementary Table 2. Primer sequences used in regular polymerase chain reaction

Gene		Sequences
<i>Hif2a</i> , for genotyping	Forward (F)	5'-CAG GCA GTA TGC CTG GCT AAT TCC AGT T-3'
	Reverse (R1)	5'-CTT CTT CCA TCA TCT GGG ATC TGG GAC T-3'
	Reverse (R2)	5'-GCT AAC ACT GTA CTG TCT GAA AGA GTA GC-3'
Promoter and 5'-UTR of	Forward	5'-GGA GGG GAG GAG GTT TTA TT-3'
<i>Epo</i> , for COBRA & BGS	Reverse	5'-CCT CAT CTC CCC AAA ATC CT-3'
Distal 5'-enhancer of <i>Epo</i> , for BGS	Forward	5'-TCA AAC AGG AAA TCC CCA GG-3'
	Reverse	5'-GAA TGT GTA CTG CTA GCC GG-3'

Supplementary Table 3. Primer sequences used in methylation-specific polymerase chain reaction of *Epo* 5'-UTR

		Sequences
Unmethylation-specific	Forward	5'-GTT GGT GGT TGT GTT TTA TTG TGT TTT T-3'
	Reverse	5'-AAA CTC CTT AAC AAC CCA AAA C-3'
Methylation-specific	Forward	5'-CGG TGG TTG TGT TTT ATT GTG TTT TC-3'
	Reverse	5'-AAA CTC CTT AAC GAC CCG AAA-3'